Proceedings of the
International Conference on Mechanical Engineering 2011
(ICME2011) 18-20 December 2011, Dhaka, Bangladesh

ICME11-FL-040

GURNEY FLAP APPLICATIONS FOR AERODYNAMIC FLOW CONTROL

M. Suresh and N. Sitaram

Thermal Turbomachines Laboratory, Department of Mechanical Engineering
IIT Madras, India

ABSTRACT

Gurney flap was developed by Dan Gurney as a lift enhancement device used to increase the down force provided by the wing of his Indianapolis-500 racecar. These small flaps, which are typically less than 0.02c in height and extend perpendicularly from the lower surface of an airfoil near its trailing edge increase the maximum lift coefficient, in some cases, by nearly 30%. A short separated region of increased pressure upstream of the Gurney flap is accompanied by two counter-rotating vortices formed downstream, effectively increasing the camber and shifting the Kutta condition to a point off of the surface of the airfoil. Gurney flaps are a practical solution for increasing lift if the accompanying increase in drag is not a significant detractor. In addition to the download wings of racecars, applications that have been considered include airfoil, wind turbine blades and turbomachinery.

Keywords: Gurney Flap, Turbomachinery, Airfoils, Wind Turbines, Aerodynamic Flow Control

.

1. INTRODUCTION

Gurney flap (GF) is named after the race car driver Dan Gurney, who first used this type of flap to increase the "down force" and thus the traction generated by the inverted wings on his race cars. GF is simply a short flat plate attached to the trailing edge perpendicular to the chord line on the pressure side of an airfoil (Fig. 1). Investigations have shown that GF increases the effective camber of the airfoil, which makes a significant increase in lift with only a small increase in drag as long as the flap height scales with the local boundary layer thickness. GF height typically ranges from less than 1% to about 5% of the chord length.

2. GF ON AIRFOILS, WINGS AND AIRCRAFT

Effect of GF on a low-speed airfoils were conducted by Liebeck [1] on a Newman airfoil, Li et al. [2] on a NACA0012 airfoil and concluded that GF is to substantially increase the maximum lift coefficient and it increases the effective camber of the airfoil and the stall angle is reduced, while the zero-lift angle of attack becomes increasingly more negative with an increase in the GF height (h). The result of such an airfoil is shown in Fig. 2. Similar results have been found for NACA4412 by Jang et al. [3-5], for NACA0011 airfoil by Myose et al. [6-9], for NACA0012 and e423 airfoil by Jeffrey et al. [10,11] and for LA203A and Gottingen 797 airfoil by Giguere et al. [12]. When the height of the GF exceeds more than 2% c the drag coefficient of airfoil abruptly increases, this was pointed by Liebeck [1], Li et al. [2] and Giguere et al. [13] with others [14-16] and suggested the optimum GF size for best lift-to-drag ratio is determined by the flow condition at the trailing edge on the pressure side of airfoil and the flap to be submerged in the boundary layer. Investigation on mounting location (s) of GF on airfoil was carried out by Li et al. [17], Yen et al. [18] and McD Galbraith [19] and found that best performance can be obtained when the GF is mounted at the trailing edge of the airfoil, Fig. 3. Studies on GF mounting angle (θ) on airfoil at 45°, 60° and 90° to the chord, Fig. 4, suggested that the inclined GFs may increase the lift-to-drag ratio by reducing the drag penalty [17, 20-22].

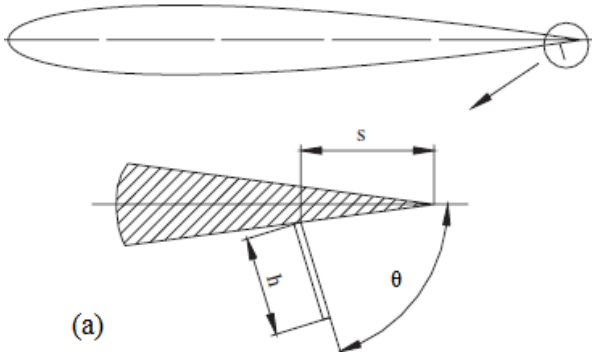

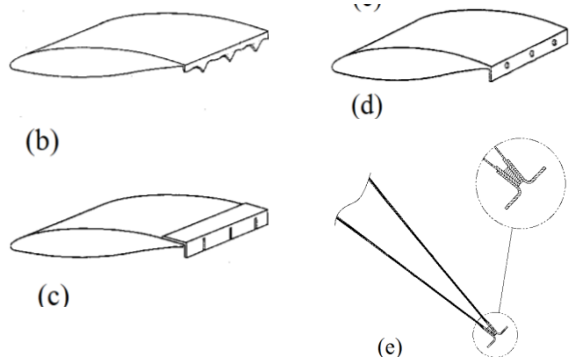

Fig. 1 Gurney Flap configurations (a) Typical GF (b) Saw toothed GF (c) GF with slits (d) Perforated GF (e) T-Strips

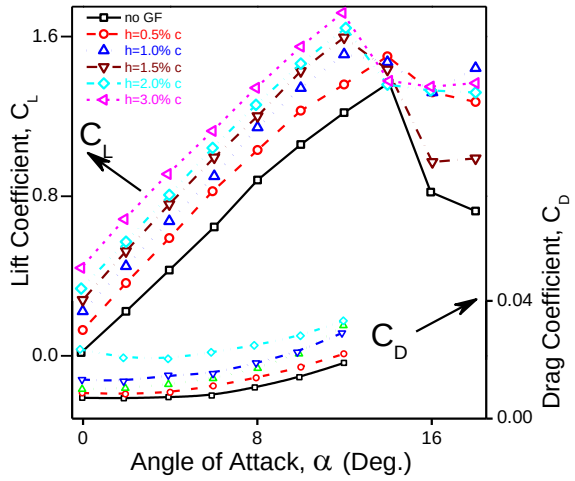

Fig 2. Variation of Lift and drag coefficient vs. angle of attack with height (h) of Gurney flap (Ref. 19)

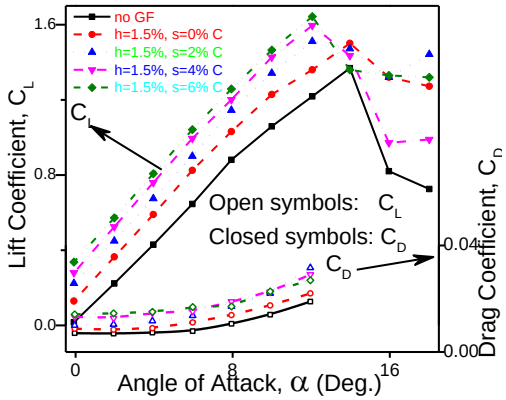

Fig 3. Lift and drag coefficient vs. angle of attack for different Gurney flap locations (Ref. 19)

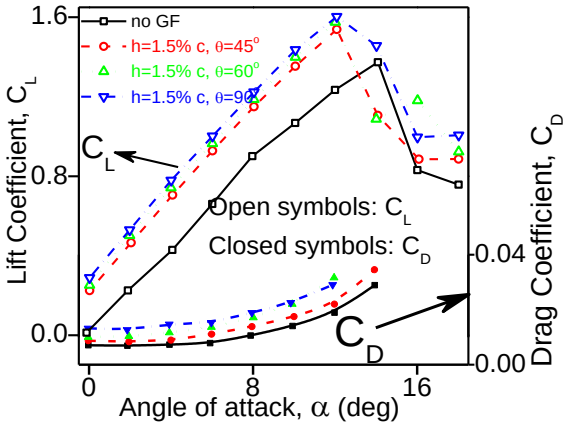

Fig. 4 Lift and drag coefficient vs. angle of attack for different flap mounting angles (Ref. 19)

Various configurations of GFs such as saw-toothed GF [14, 23-25], GFs with slits, holes, vortex generators [26] and perforated GF [27] were investigated and airfoil aerodynamics showed that these flaps can make the flow around the trailing edge more three-dimensional. These configurations moved the separation point forward over the upper surface of the airfoil with increasing the lift and reducing the drag as compared to a plain GF of same height.

An excellent review of their scope of application in airfoils, wings and aircraft is given by Wang et al. [28]. A combination of the Gurney flap with the trailing edge flap showed additional lift enhancement coupled with a reduction in lift-to-drag performance [29]. Colman [30] concluded Gurney flap enhance the lift coefficient of the airfoil, and that its performance is almost independent of the scales of the incoming turbulence. The tests were performed at turbulence intensity of 1.8% and 3.5% and at a Reynolds number of $3x10^5$. Cavanaugh et al. [31] carried out a wind tunnel test on a NACA 23012 wing of aspect ratio 6 equipped with Gurney flaps and trailing edge T-strips at Reynolds numbers of $1.95x10^6$, $1.02x10^6$ and $0.51x10^6$. T-strip heights of 0.42%, 1.04%, 1.67%, 2.08%, 2.92%, 4.17% and 5.00% chord were tested and concluded that T-strips produced an increase in the slope of the lift curve and an increase in maximum lift coefficient, but produced no shift in the wing zero-lift angle of attack. T-strips also produced a rearward shift in the wing aerodynamic center, but produced no increment in the pitching moment coefficient near zero lift.

GFs have proved to be very efficient and effective passive device in improving the lift characteristics of airfoil, but the mechanisms responsible for this have not been understood completely. As a part to throw light on this, pressure and velocity measurement on airfoil surface as well as PIV measurement and die-injection flow visualization has been carried out by various researchers [1-3, 6, 9, 14, 33-34]. Instantaneous flow patterns around the GF show a wake containing an alternatively shed Karman vortex sheet. The time averaged velocity profile concluded that the wake downstream the flap consisting of a pair of counter-rotating vortices is turned downwards (Fig. 5a). It also shows the presence of an off-surface stagnation point downstream of the trailing edge. The presence of a pair of counter-rotating vortices downstream the GF results

in low pressure there, which reduces the adverse pressure gradient near the trailing edge of the airfoil. This leads to a delay or elimination of flow separation over the upper surface of the airfoil (Fig. 5 (b)) accompanied by a reduction in the boundary layer thickness. The vortices also increase the velocity over the upper surface, which in turn increase the suction on the rear body. On the other hand, the flow velocity upstream of the GF is reduced and the pressure on the lower surface of rear body is thus increased. The net effect of suction increase on the upper surface and pressure increase on the lower surface leads to an increase in the total circulation of the airfoil, giving rise to a lift enhancement by the GF. A NACA 4412 airfoil was tested, in a boundary layer wind tunnel, with the aim to study the effect of a moving (oscillating) Gurney flap, as an active and passive flow control device submitted to a turbulent flow field [35]. The results obtained, show us that the oscillating GF change the wake flow pattern, alleviating the near wake turbulence and enhancing the vortex pair near the trailing edge at the mini-flap level and below that level, magnifying the effect described by Liebeck [1]. That effect is more evident as the oscillating frequency grows.

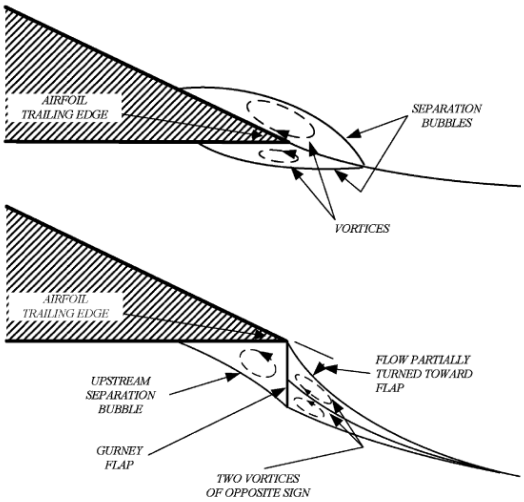

Fig. 5a) Flow pattern without and with the GF [Ref. 1]

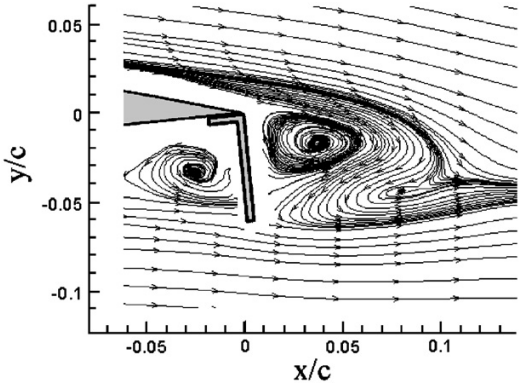

Fig. 5b) Time-averaged streamlines with 6% C GF at α=2.5^o [Ref. 34].

3. APPLICATION OF GF IN TURBOMACHINES

3.1 Axial compressor and fan

Many axial fan types operate at relatively low Reynolds numbers due to their relatively small chord lengths or relatively low rotational speeds in their applications. These are used for ventilation, cooling, vacuuming and dust removal, etc. and consume a large fraction of industrial energy. These fans generally operate at near-atmospheric conditions, and this result in fan blade Reynolds numbers which ranges from a few thousand to approximately 10^5. In this range conventional airfoils or blade profiles perform poorly due to laminar separation, which in turn affect the performance, efficiency and the power consumption of the machine.

Janus [36] conducted a computational study on linear cascade of an industrial fan for GFs between h=0.5% and 2% of the blade chord and concluded that GF of 1% of the blade chord produced the best overall performance improvement. Myose et al. [37] flow visualization study on a low Reynolds number (Re=16,000) NACA 65-(12)10 compressor cascade with Gurney flaps with h= 2% of the chord length attached to the trailing edge of the cascade blades concluded that the Gurney flap energizes the flow and delays the stall at large incoming flow angles. As Gurney flaps are effective at low Reynolds number, Greenblatt [38] experimentally investigated GF on a 150 Watt ventilation fan with 394 mm nominal blade diameter. The blades had a span of 147 mm, a root chord of 84 mm and tip chord of 70mm. Tests were conducted at a fan speed of 1200 rpm for flap configuration and height of 10%c thin, 10%c thick, 20%c thin, 20% composite and 30%c thick. Reynolds number varied approximately from 25000 near the hub to 115000 at the tip at design condition and these values were 20% lower at the off-design condition.

From performance analysis of the fan i.e. pressure rise (Δp) vs. volumetric flowrate (Q), (Fig. 6), it can be noted that at low flowrates (0.07 $m^3/s \leq Q < 0.1 m^3/s$), GF indicated pressure decreases that are steeper with increasing Q than the baseline case (no GF). With further increase in flowrate, this trend changes and pressure decreases less rapidly than the baseline case. The trend is similar to airfoil with GF; under stalled (low Q) and pre-stalled (higher Q) flow regimes [28]. At low Q where fan blades are fully stalled, the lift force or the pressure difference across the blades does not change significantly with angle of attack (i.e., increasing Q).The addition of GFs increases lift but mainly increases drag, and hence, the blade drag dominates the performance as a function of Q. With increasing Q, the blade move to the prestall regime, resulting in improved performance of the flaps and hence a small pressure drop across the blade row with increasing Q. This occurs irrespective of the thickness of the flap. At even larger Q, with blades fully in the prestall regime, the performance remains superior to the baseline case. Figure 7 shows the variation of Energy coefficient (ψ) with Flow coefficient (ϕ) for different GF configuration at design condition and off-design conditions.

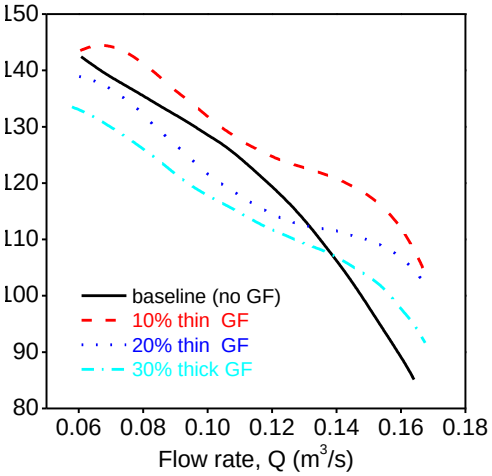

Fig 6. Fan pressure developed as a function of volumetric flowrate at design condition [Ref. 38].

It can be noted that GF produced higher ψ for the entire range of ϕ when compared to baseline values and at, off-design condition GF of larger size were favorable due to the lower Reynolds numbers. Not only are flapped blades Energy coefficients substantially higher than the baseline but the rate at which they are decreasing also decrease with flap size. Fan static efficiency for the baseline and flap configurations is shown in Fig. 8 for design condition and can be noted that all flapped configurations produced lower efficiency at low flowrates but in each case, the peak efficiency exceeded that of the baseline case. The 10% thin flap produced the largest increase of 18% in static efficiency, while flap mass, relative to the mass of the blade was seen to be an important parameter. Based on the observation made by Greenblatt, implementation of GF on the fan blade can potentially reduce sound pressure level and for his case it reduced by 4 dB. Similar effort to reduce the noise of axial fan using a GF is reported by Yongwei [39].

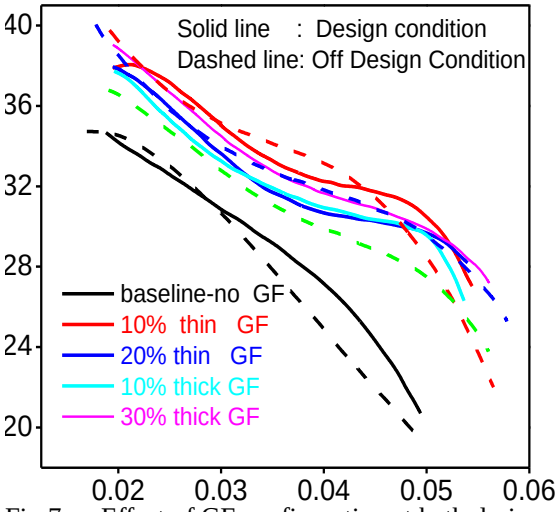

Fig 7. Effect of GF configuration at both design and and off-design conditions [Ref. 38].

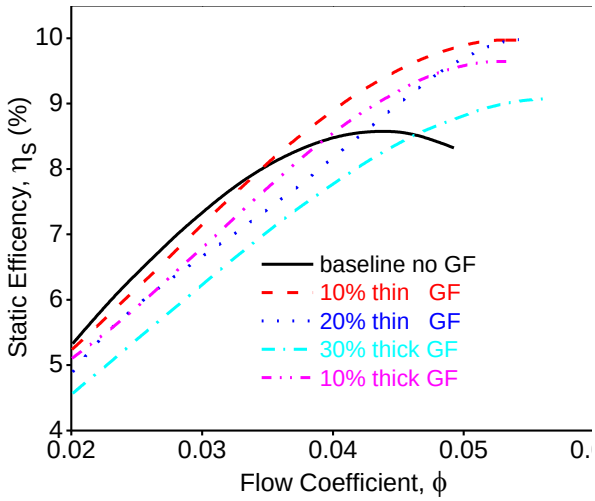

Fig 8. Effect of GF on fan static efficiency as a function of flow coefficient, at design condition [Ref. 38].

3.2 Centrifugal fan

Centrifugal fans are finding their applications in low Reynolds number flows as they need to be operated at low speeds for cooling electronic devices, refrigeration fans, air conditioning fans, etc. Due to their low rotational speeds in these applications, they end up in lower efficiency. As an effort to increase its performance at low Reynolds number, Manoj Kumar et al. [40] experimentally investigated the effect of GF on a low specific speed centrifugal fan impeller. Design details of the centrifugal fan tested is given in Table 1. Performance test was carried out on the fan with vaneless diffuser at five different Reynolds numbers based on the impeller blade height at exit viz., 0.82, 0.62, 0.55, 0.41, 0.30×10^5 i.e., at five speeds respectively at 3000, 2500, 2000, 1500 and 1100 rpm with and without GF. Static pressures on the vaneless diffuser hub and shroud were also measured for each speed at four flow coefficients, ϕ=0.23 (below design flow coefficient), ϕ=0.34 (design flow coefficient), ϕ=0.45 and 0.60 (above design flow coefficient). A brass angle of 1/8th inch side (3.175 mm) is used as GF on the pressure surface of the impeller blade tip. The height of the GF corresponded to 15.9% of impeller blade height at the exit or 5.1% of blade spacing at the impeller tip.

Table1: Geometric details of the centrifugal fan

Pressure ratio, P_{02}/P_{01}	1.08
Mass flow rate, m	0.56 kg/s
Speed, N	3,000 rpm
Shape number, N_{sh}	0.076
Inducer hub diameter, D_{1h}	110 mm
Inducer tip diameter	225 mm
Blade angle at inducer hub, β_{1h}	45^o
Blade angle at inducer tip, β_{1t}	29^o
Impeller exit diameter, D_2	393 mm
Number of impeller blades	20
Blade angle at exit, β_2	90^o
Blade height, h	20 mm
Exit diameter of vaneless diffuser, D_3	600 mm
All angles are w.r.t. tangential direction	

Figure 9 shows the effect of GF on the performance of the centrifugal fan at various Reynolds numbers. The qualitative difference in the performance curves without and with GFs can be observed. Energy coefficient increases with GFs for almost complete flow coefficient range and the increases is dominant at low Reynolds numbers, whereas only small increase is found in case of higher Reynolds numbers. It was also observed that maximum volume flow also increased slightly with GFs. The radial variation of static pressure coefficient on the diffuser hub and shroud is compared without and with Gurney flaps for respective flow coefficients and speeds in Fig. 10. In general static pressure on the diffuser hub and shroud is higher with Gurney flaps compared to the basic configuration of without Gurney flaps. However the difference is reduced as the Reynolds number increases with almost negligible difference at the speed of 2,500 rpm corresponding to a Reynolds number of 0.69×10^5. The results of static pressure correspond well with those of performance characteristics.

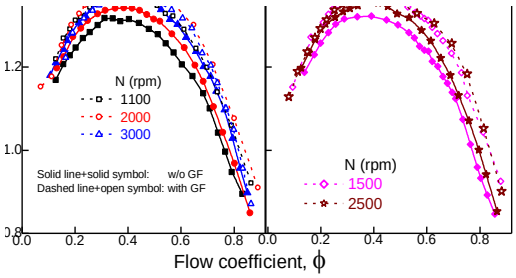

Fig. 9 Comparison of energy coefficient of the centrifugal fan without and with GF [Ref. 40]

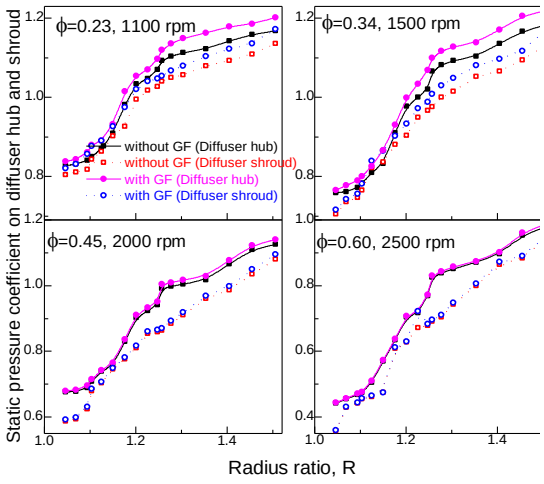

Fig. 10 Effect of Gurney flap on static pressure on diffuser hub and shroud [Ref.40]

3.3 Low pressure turbine cascade

Byerley et al. [41] and Chen et al. [42] investigated GF as a passive flow control device over a Low Pressure Turbine (LPT) blade. LPT Reynolds numbers often result in significant regions of laminar flow on the suction sides of airfoils, which makes them susceptible to the laminar separation that may or may not reattach. Laminar separation bubbles generally exist on the suction surface of LPT blade, with short bubbles slightly and long bubble notably impacting on the performance of blade. The key to maintain the aerodynamic performance of highly-loaded LPT blade is to control the laminar separation bubble on the suction surface.

Byerley et al. [41] carried out experiments on Langston turbine blade in a linear cascade with and without GF for Reynolds numbers of 28×10^3, 65×10^3 and 167×10^3. Cascade parameters are listed in Table 2. Laser thermal tufts technique was used for five different GF sizes while maintaining the inlet Reynolds number at 28×10^3.

Figure 11 shows that the effect of increasing the GF height is to move the separation further downstream. For the 2.7 mm GF, the location of separation is moved back to s/B_x=1.36 and reattached at s/B_x=1.50 and 3.9 mm successfully eliminates the laminar separation bubble.

Table 2: Cascade Parameters

Operation	Closed Loop
Axial Chord (B_x)	171 mm
Blade Pitch (p)	163 mm
Inlet Blade angle	44°
Exit Balde angle	26°
Pitch/ Axial Chord	0.95
Span/ Axial Chord	3.86
Air Inlet Angle	46°
Air Exit Angle	26°
Hydraulic radius of blade row exit (Rh)	71.5 mm

Figure 12 shows wall static pressure distribution for a blade and profile losses with and without GF at the three Reynolds number. Wall static pressure distribution for the 'no GF' cases, the terraced region moved upstream and decreased in size as Reynolds number increased. There appeared to be a very small terraced region at s/B_x=1.05 for $Re=167 \times 10^3$, since flow is attached at this point. For all Reynolds number, GF increased the exit velocity over the uncovered region of the suction surface by approximately 14% and this lead to increase lift force by 9%.

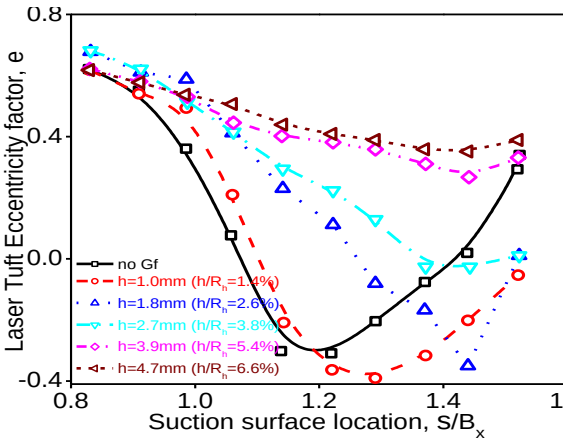

Fig 11. Effect of GF height on boundary layer separation as indicated by laser tuft eccentricity (positive values of e indicate attached flow) [Ref. 41]

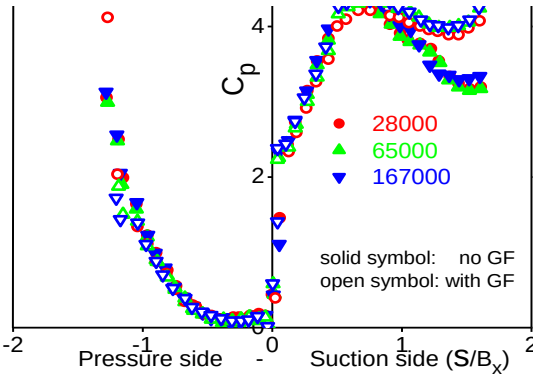

Fig 12. Effect of GF on wall static pressure at various Reynolds number [Ref. 41]

Profile loss measurements made for each of the test cases (Fig. 13) indicated that, without GF, the centre of the wake is offset to the suction side because of the thicker boundary layer on that side. The effect of GF was to shift the wake centre closer to the trailing edge camber line and to widen the wake region.

Figure 14 shows average loss coefficient plotted against Reynolds number and these values matched that predicted by Ainley correlation given in Horlock [43]. As Reynolds number increased, the losses for the plain blade dropped while, with GF, the losses at high Reynolds number were much greater. The GFs turned the flow approximately 0.8 deg towards the direction of the suction surface of the neighboring blade.

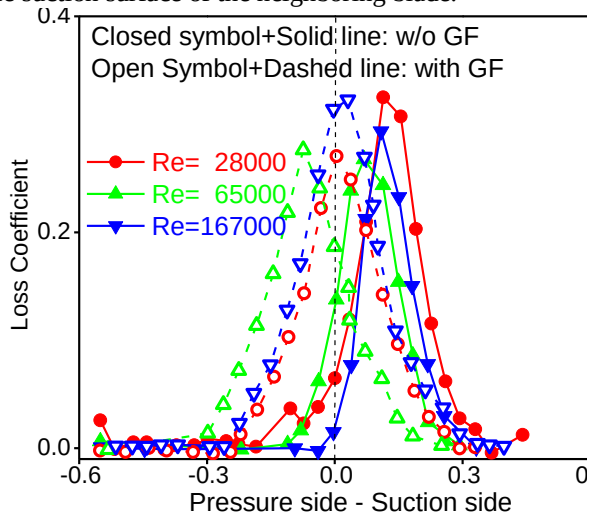

Fig 13. Effect of GF on profile losses at various Reynolds numbers [Ref. 41]

Numerical simulations were performed by Chen et al. [42] on three turbine cascades with same profile and different solidity, namely Pack B, Pack LB-I and Pack LB-II. The pitch-chord ratio of Pack B is 1.25, relative to which solidity of Pack LB-I and Pack LB-II were decreased 12.5% and 25% respectively. Three types of GF geometries, Square, Rectangle and Smooth Concave GFs were investigated at the trailing edge on the pressure side of the cascade as in Fig. 15 at three Reynolds numbers ($Re=2.5\times10^4$, $Re=1.0\times10^5$ and $Re=2.0\times10^5$). Effect of GF normalized height (H=h/C) on energy loss coefficient and cascade flow turning angles indicated that energy loss coefficient firstly decreases then increases with the increase of the flap height, but at higher Reynolds numbers the energy loss coefficient increases with H. This means GF with appropriate height can reduce the boundary layer separation and associated flow losses on the adjacent blade suction side and the flow turning angle increased with increase of flap height which agreed with Byerley et al. [41]. Figure 16 shows the variation of energy loss coefficient and flow angle with Reynolds numbers for Pack LB-I cascade, indicating that Round GF is the most effective to increase the flow turning angle and reduce the flow losses in the low-solidity cascade.

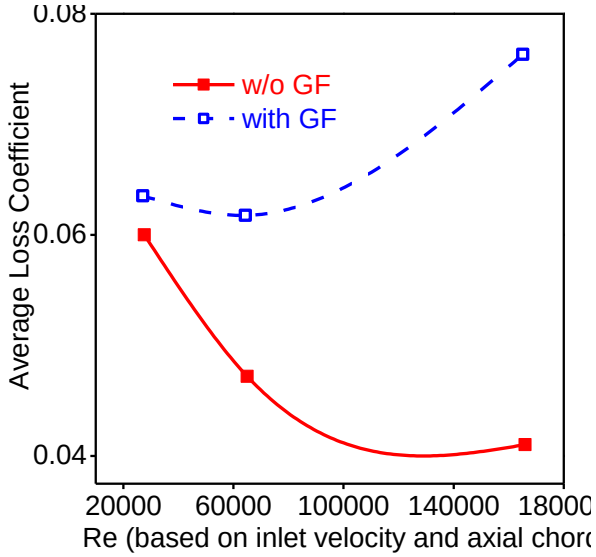

Fig 14. Effect of GF on average profile loss as a Function of Reynolds number [Ref. 41]

As a result larger turning angle of the flow caused by GF corresponds to better effectiveness of GF, thus it can be concluded that for low-solidity cascades, the effectiveness difference between different GF types mainly depends on the deflection of the main stream caused by GF. With GF the adverse pressure gradient can be weaken due to the deflection of the main stream caused by the flap, which thins the separation bubble and delays the transition onset, contributing to reductions of both the separation-bubble-generated loss and the turbulent boundary-layer-generated loss.

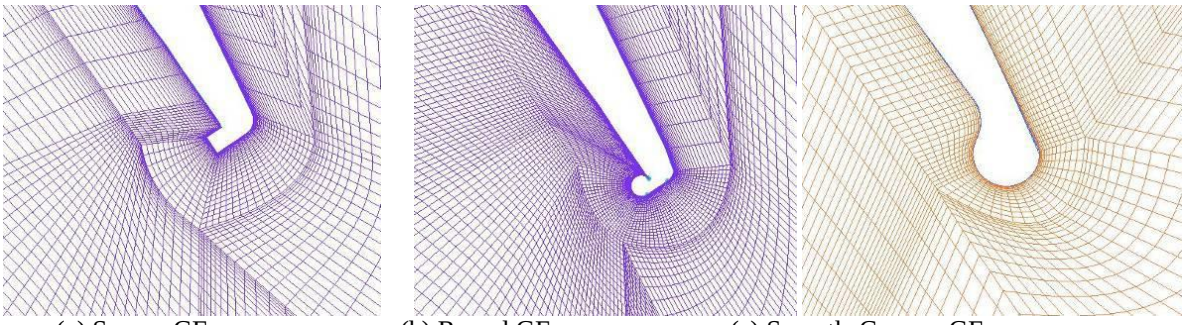

(a) Square GF (b) Round GF (c) Smooth-Convex GF

Fig. 15 Schematic of types of Gurney flaps [Ref. 42]

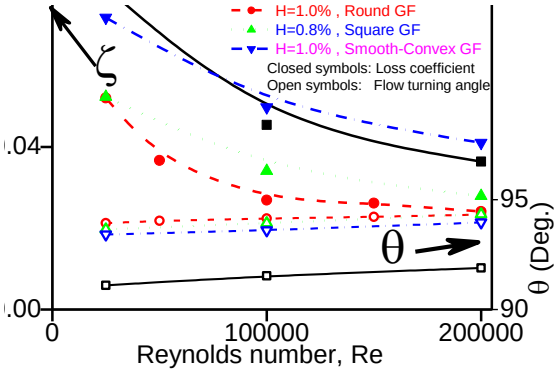

Fig. 16 Energy loss coefficient and flow turning angle vs. Reynolds number (Re) [Ref. 42]

3.4 Wind turbines

To reduce the loads and/or increase the performance of modern wind turbines, many passive flow control and Active flow control solutions are used such as Flexible Trailing Edge Flap, Gurney Flap & Micro Tabs, Stall Rib and Flexible Leading Edge Flap. With all these flow controls devices available Gurney flaps are better for performance increment, load reduction, power regulation, operating conditions, cost and maintenance. For stall controlled wind turbines, the power production is limited both at low and high wind conditions. When the wind speed is very low, conventional wind turbines generate little or no usable power. This has limited the deployment of wind turbines to a relatively small number of sites where favorable conditions exist. At the other extreme, when the wind speeds become very high, the rotor invariably stalls and experiences highly unsteady aerodynamic forces and moments. This limits the use of stall regulated rotors to lower wind speeds where the flow is mostly attached, thereby limiting the useful operating range of the rotor. Over the past several years, there has been an increased effort to extend the usable operating range of stall regulated wind turbines.

Gurney flaps are sometimes used at the inner part of a wind turbine blade to increase the pressure difference across the trailing edge and thereby the amount of lift coefficient at a given angle of attack.

Van Dam [44] based on the research of Bechert et al. [45] investigated the effects of serrated and slit GFs (i.e. micro tabs) to eliminate the 2D vortex shedding from the solid GFs which can cause vibration and noise. Additionally van Dam et al. [46] investigated the implementation of Micro Flaps (i.e. active GFs) and deployable Micro Tabs as means for load alleviation in wind turbine blade structures. It was found, both micro alleviation mostly due to their fast actuation capabilities. The main difference between these two configurations is the slight aerodynamic lag of the micro tabs due to their position. The actuating mechanism in the case of micro flaps requires low actuation force due to the small size of the element. Alternatively the implementation of sinking micro tabs [46] could further simplify the actuation process. The integration of Gurney flaps and Micro Tabs in the blade structure is a relatively simple process. These elements and their actuators are very small; therefore only minor changes need to be made in the current blade structures. Especially in the case of Micro Flaps (i.e. active GF), the flap mounting point can easily be integrated at the trailing edge region of the blades and the actuators could be mounted externally without significant aerodynamic penalties for the blade. To achieve a significant load reduction during the operation of the wind turbine a fast and reliable control and actuation system is needed. From the aerodynamic and mechanical point of view GFs and Micro tabs are suitable for fast control and actuation.

Kentfield [47-49] installed the GFs on NACA0015, NACA0020 and NREL S809 airfoils to verify that the wind turbine efficiency can be improved by them and the experiment indicated that wind turbine output power cab be increased for wind speeds greater than 8.5 m/s. Timmer et al. [50] investigated the effect of GFs of 1%c (6 mm) and 2%c (12 mm), the effect of isosceles wedges of 1%, 1.5%, and 2% height and of upstream length of the 1%c high wedges on wind turbine dedicated Airfoil DU 93-W-210, at a Reynolds number of 2×10^6. GFs and wedges investigated are shown in Fig. 17. With the 1%c and 2%c Gurney flap, the maximum lift coefficient was increased by 0.24 and 0.40, respectively. The maximum lift-to-drag ratio, however, decreased from 136 to 117 and 89, respectively. The test results showed that there was virtually no difference between the characteristics for the 6×6 mm. wedge and the 6 mm high Gurney flap. Apparently the 6×6 mm wedge filled the space otherwise taken by the separation bubble in front of the Gurney flap. It followed that with increasing upstream wedge length the maximum lift coefficient decreased while the maximum lift-to-drag ratio increased. The wedges with a longer upstream length have a smaller effect on the airfoil camber, but at the same time redirect the flow with less base drag. Pechlivanoglou et al. [51] investigated the three GF configurations shown in Fig. 17 and a serrated GF on a DU96W180 airfoil and the results shown in Fig. 18 conclude that all GF configurations offer a very attractive AFC solution for wind turbine applications

mostly due to their relatively high aerodynamic control and dynamic (unsteady)

experiment proved that the load reduction potential of such an AFC system is considerably high.

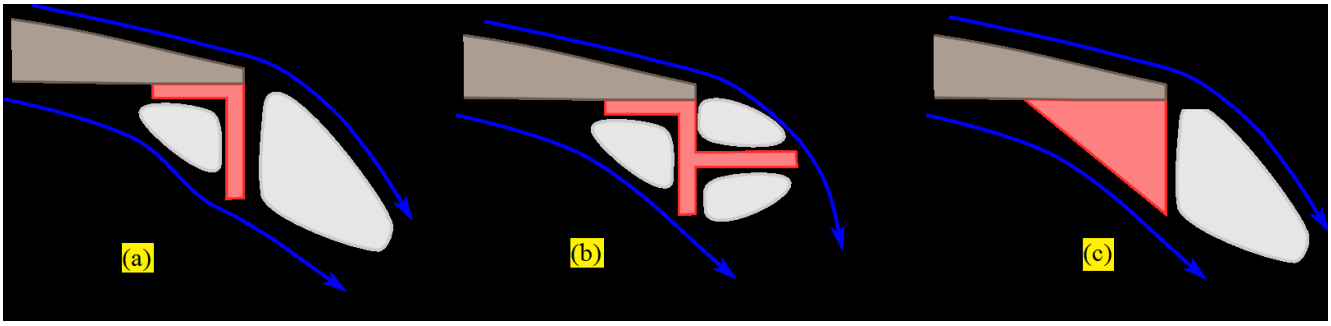

(a) Typical GF (b) GF with splitter plate (c) Wedge shape GF

Fig. 17 Some GF configurations tested in wind turbine blades [Ref. 51]

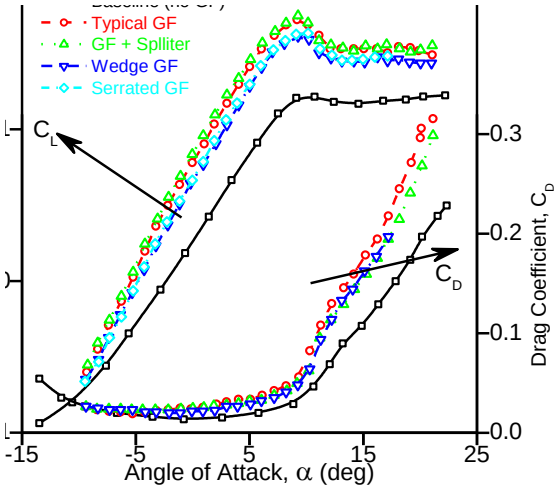

Fig 18. Variation of lift and drag coefficients for different GFs on a DU96W180 airfoil [Ref. 51]

Fuglsang et al. [52] experimented with vortex generators and GFs in combination on Risø-B1 airfoil family for MW-size wind turbines at a Reynolds number of 1.6×10^6 and concluded that vortex generators and GFs in combination increase the maximum lift coefficient of 34% to 2.17, making vortex generators and Gurney flaps an attractive option for the root of a wind turbine blade. Nengsheng et al. [53] experimentally studied the power and efficiency augmentation of the horizontal axis wind turbine on a NACA 63_2-215 airfoil at a Reynolds number of $2.4\text{x}10^5$, based on airfoil chord with GF and trailing edge flaps. In experiments the angles of attack varied from 0° to 40° and the heights of the flaps are 1.0%, 1.5%, 2.0% and 2.5%c. The effects of different deflection angles (0°, 45°, 90°, 135°) of the trailing edge flap were compared. The results indicate that all tested flaps could increase the lift coefficient and the larger flaps produce successively larger increments, although not proportionally. The Gurney flap shows a superior performance compared with other angles trailing edge flaps.

Zhang et al. [54] and Zhao et al. [55] carried out numerical investigation on a vertical axis wind turbine (NACA0015 airfoil) and horizontal axis wind turbine (FFA-W3-241 airfoil) with GFs resulted that Gurney flap can improve the lift coefficient of the airfoil and the height of the flap plays an important role. At the same time, output power of the wind turbine with Gurney flap increases compared with wind turbine without flap, and range of tip speed ratio to increase the wind power efficient broaden, which is useful for control and adjustment of wind turbine. Zhu et al. [56] experimental investigations on the performance of horizontal axis wind turbine of FFA-W3-211 airfoil with a GF of h=4%c; pitch angles of the blade were between 4^o~14^o and tested at wind speeds between 8~14 m/s. Results show that GF has significant effects on the wind turbine performance, especially at large pitch angles compared to small pitch angles and these increased the power of the wind turbine by over 38% at a pitch angle of 12^o. Tongchitpakdee [57] numerically investigated Gurney flap in horizontal axis wind turbine rotor at a wind speed of 7 and 15m/s with 0, 10 and 30 deg yaw angles. Results indicated that the radial variation of normal force coefficient C_N and tangential force coefficient C_T (Fig. 19) increases with GF at 7m/s while the effect seems to be less at 15m/s. Increase in C_N leads to increase in lift while increase in C_T due to GF increases torque generated, which can be seen in Fig. 20. At a wind speed of 15m/s, extensive separation occurred on the rotor. It can be seen that the GF has a negligible influence on the flow field, under this separated flow condition. The use of Gurney flap thus results in only a small increment of the normal and tangential force components (Fig. 19) and on the production of shaft torque or power (Fig. 20).

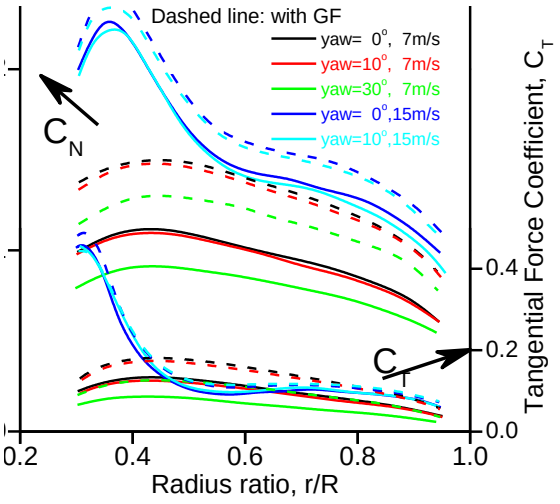

Fig 19. Radial distribution of normal force coefficient C_N and tangential force coefficient C_T at 7m/s and 15m/s; with and without a GF [Ref. 57]

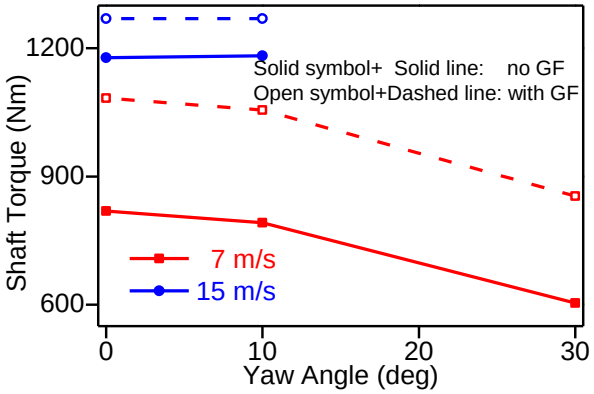

Fig 20. Variation of shaft torque as a function of yaw angle with and without GF [Ref. 57]

4. CONCLUSIONS

The GFs can increase the lift coefficient of airfoils, wings and aircrafts both at subsonic and transonic speeds, and hence their aerodynamic performance can be significantly improved. They have shown that they have a significant role to play at low Reynolds number operations of turbomachines such as axial and centrifugal fan, low pressure turbine and wind turbines. GF on an axial fan increases performance of the fan and at the same time reduces the power consumption and reduces the fan noise. Static efficiency of the axial fan is relatively high with a GF than the baseline. Centrifugal fan energy coefficient increase with GF at low Reynolds number however the effect seems to be less at higher Reynolds number. They even increase the static pressure on the diffuser hub and shroud of centrifugal machines and have shown to have an effect on operating range. GFs are very successful in eliminating the laminar separation bubble for low Reynolds numbers operation on a LP turbine blade and shown a significant effect on loss coefficients. GFs turn the flow on a blade towards the direction of the suction surface. The centre of the wake region is shifted from suction surface side towards the pressure surface when the GFs are installed. Like many flow control devices available for a wind turbine blade, GFs are better in terms of performance increment, load reduction, power regulation and stall control.

5.NOMENCLATURE

Symbol	Meaning	Unit
c	Chord length of an airfoil	(m)
C_D	Drag coefficient	
C_L	Lift coefficient	
C_N	Normal force coefficient	
C_P	Pressure coefficient	
C_T	Tangential force coefficient	
e	laser tuft eccentricity factor	
H	Normalised Gurney flap height (h/c)	
h	Gurney flap height	(m)
Q	Flowrate	(m^3/s)
s	Mounting distance (to the trailing edge)	(m)
s/B_x	Suction surface location	
α	Angle of attack	(Deg.)
Δp	Pressure rise	(Pa)
ϕ	Flow coefficient	
θ	Mounting angle	(Deg.)
η_S	Static efficiency	

ψ	Energy coefficient	

6.REFERENCES

1 Liebeck RH, 1978 “Design of subsonic airfoils for high lift”, J Aircr ;15(9):547–61.

2 Li YC, Wang JJ, Zhang PF, 2002 “Effect of Gurney flaps on a NACA0012 airfoil”, Flow Turbul Combust;68(1):27–39.

3 Storms BL, Jang CS,1994 “Lift enhancement of an airfoil using a Gurney flap and vortex generators” ,J Aircr;31(3):542–7.

4 Jang CS, Ross JC, Cummings RM, 1998 “Numerical investigation of an airfoil with a Gurney flap”,Aircr Des;1:75–88.

5 Jang CS, Ross JC, Cummings RM, 1992 “Computational evaluation of an airfoil with a Gurney flap”, AIAA paper 92-2708.

6 Myose R, Heron I, Papadakis M, 1996 “Effects of Gurney flaps on a NACA0011 airfoil”, AIAA paper 96-0059.

7 Myose R, Papadakis M, Heron I, 1997 “A parametric study on the effect of Gurney flaps on single and multi-element airfoils, three-dimensional wings and reflection plane model”, AIAA paper 97-0034.

8 Myose R, Papadakis M, Heron I, 1998 “Gurney flap experiments on airfoils, wings, and reflection plane model”, J Aircr;35(2):206–11.

9 Myose R, Heron I, Papadakis M, 1996 “The post-stall effect of Gurney flaps on a NACA0011 airfoil”, SAE paper 961316.

10 Jeffrey DR, Zhang X, Hurst DW, 2000 “Aerodynamics of Gurney flaps on a single-element high-lift wing”, J Aircr;37(2):295–301.

11 Jeffrey DR, 1998 “An investigation into the aerodynamics of Gurney flaps”, PhD thesis, Department of Aeronautics and Astronautics, Faculty of Engineering, University of Southampton.

12 Giguere P, Lemay JM, Dumas G, 1995 “Gurney flap effects and scaling for low-speed airfoils”, AIAA paper 95-1881.

13 Giguere P, Dumas G, Lemay J, 1997 “Gurney flap scaling for optimum liftto-drag ratio”, AIAA J;35(12):1888–90.

14 Neuhart DH, Pendergraft OC, 1988 “A water tunnel study of Gurney flaps”, NASA TM-4071.

15 Storms BL, Jang CS, 1993 “Lift enhancement of an airfoil using a Gurney flap and vortex generator”, AIAA paper 93-0647.

16 Selig MS, Monovan JF, Fraser DB, 1989 “Airfoil at low speeds” Virginia Beach, VA, 23451: SoarTech 8, SoarTech Publications, 1504N, Horseshoe Circle; 1989. p. 73–75.

17 Li YC, Wang JJ, Zhang PF, 2003 “Influences of mounting angles and locations on the effects of Gurney flaps” J Aircr;40(3):494–8.

18 Yen DT, van Dam CP, Brauchle F, Smith RL, Collins SD, 2000 “Active load control and lift enhancement using MEM translational tabs” AIAA paper 2000-2242.

19 McD Galbraith RA, 1995 “The aerodynamic characteristics of a GU25-5(11)-8 airfoil for low Reynolds numbers” Exp Fluids 1985;3:253–6.

20 Bloy AW, Durant MT, 1995 “Aerodynamic characteristics of an aerofoil with small trailing edge flaps” Wind Eng;19(3):167–72.

21 Bloy AW, Harrison DF, 1998 “Free-stream turbulence effect on Gurney type flaps” Wind Eng 1998;22(3):149–58.

22 Traub LW, Miller AC, Rediniotis O, 2006 “Preliminary parametric study of Gurney flap dependencies” J Aircr;43(4):1242–4.

23 Vijgen PMHW, van Dam CP, Holmes BJ, 1989 “Wind-tunnel investigations of wings with serrated sharp trailing edges” Proceedings of the conference on low Reynolds number airfoil aerodynamics, University of Notre Dame, USA; p. 295–313.

24 van Dam CP, Yen DT, Vijgen PMHW, 1999 “Gurney flap experiments of airfoil and wings” J Aircr;36(2):484–6.

25 Li YC, Wang JJ, Zhang PF, 2003 “Experimental investigation of lift enhancement on a NACA0012 airfoil using plate/serrated Gurney flap” Acta Aeronaut Astronaut Sin;24(2):119–23

26 Meyer R, Hage W, Bechert DW, Schatz M, Thiele F, 2006 “Drag reduction on Gurney flaps by three-dimensional modifications” J Aircr;43(1):132–40.

27 Lee, T, 2009 “Aerodynamic Characteristics of airfoil with Perforated Gurney-Type Flaps” J Aircr, Vol. 46, No. 2, p. 542-548.

28 Wang, J. J., Li, Y. C., and Choi, K.-S., 2008 “Gurney Flap: Lift Enhancement, Mechanisms and Applications“ Prog. Aerosp. Sci., 44, pp. 22–47.

29 Lance W. Traub and Adrian Akerson, 2010 “Airfoil Lift Augmentation at Low Reynolds Number”, J Aircr, Vol. 47, No. 6.

30 J.Colman, J. Maranon di leo, J. S. Delnero, M. Martinez, U. Boldes and F. Bacchi, 2008 “Lift and drag coefficient behavior at low Reynolds Number in an Airfoil with Gurney Flap Sumitted to a Turbulent Flow. Part 1”, Latin American Applied Research, 38:195-200.

31 Michael A. Cavanaugh, Paul Robertson and William H. Mason, 2007 “Wind Tunnel Test of Gurney Flaps and T-Strips on an NACA 23012 Wing” 25th AIAA Applied Aerodynamics Conference, AIAA 2007-4175.

32 Liu TS, Montefort J, 2007 Thin airfoil theoretical interpretation for Gurney flap lift enhancement. J Aircr;44(2):667–71.

33 Troolin DR, Longmire EK, Lai WT, 2006 Time resolved PIV analysis of flow over a NACA0015 airfoil with Gurney flap. Exp Fluids;41(2):241–54.

34 Gai SL, Palfrey R, 2003Influence of trailing-edge flow control on airfoil performance. J Aircr;40(2):332–7.

35 Mauricio E. Camocardi, Julio Maranon Di Leo, Juan S. Delnero and Jorge L. Colman Lerner, 2011 “Experimental Study Of A Naca 4412 Airfoil With Movable Gurney Flap”, 49th AIAA Aerospace Sciences Meeting including the New Horizons Forum and Aerospace Exposition; AIAA 2011-1309.

36 Janus, J. M., 2000 “Analysis of Industrial Fan Designs with Gurney Flaps”, AIAA Paper No. 2000-983.

37 Myose, R. Y., Lietsche, J. C., Scholz, D., Zinge, H., Hayashibara, S. and Heron, I., 2006 “Flow Visualization Study on the Effect of a Gurney Flap in a Low Reynolds Number Compressor Cascade”, AIAA Paper 2006-7809.

38 Greenblatt, D., 2011 “Application of Large Gurney Flaps on Low Reynolds Number Fan Blades”, ASME Journal of Fluids Engineering, 133, pp. 021102-1 to 021102-7.

39 Gao Yongwei, 2006 “Simple Method Using Gurney Flap to Reduce Noise of Axial Fan”, Compressor, Blower & Fan Technology, Issue 2, pp. 15-16.

40 Manoj Kumar Dundi, T., N. Sitaram, M. Suresh, 2011 “Application of Gurney Flaps on a Centrifugal Fan Impeller”, accepted for presentation at the 11th Asian International

Conference on Fluid Machinery and publication in the proceedings, Nov. 21-23, 2011, Chennai, India.

41 Byerley, A. R., Störmer, O., Baughn, J. W., Simon, T. W., Van Treuren, K. W., and List, J., 2003 "Using Gurney Flaps to Control Laminar Separation on Linear Cascade Blades", ASME Journal of Turbomachinery, Vol. 125, No. 1, pp. 114–120.

42 Chen, P. H., Qiao,W-Y. and Luo, H-L., 2010 "Investigation of low solidity LP turbine cascade with flow control: Part 2–Passive flow control using Gurney flap", ASME Paper GT2010-22330.

43 Horlock, J. H., 1966, *Axial Flow Turbines*, Butterworths Publishing Company, London.

44 Chow, R., and van Dam, C. P., 2007. "Computational investigations of small deploying tabs and flaps for aerodynamic load control". Journal of Physics, 75, p. 11.

45 D.W. Bechert, R. M., and Hage, W., 2000. "Drag reduction of airfoils with miniflaps. what can we learn from dragonflies". AIAA (Fluids 2000), p. 30.

46 Mayda, E., and van Dam, C., 2005. "Computational investigation of finite width microtabs for aerodynamic load control". AIAA, p. 13.

47 Kentfield JAC, 1993 The flow physics of Gurney flaps, devices for improving turbine blade performance. Wind Eng;17(1):24–34.

48 Kentfield JAC, 1994 Theoretically and experimentally obtained performances of Gurney flaps equipped wind turbines. Wind Eng; 18(2):63–74.

49 Kentfield JAC, 1996 Influence of free-stream turbulence intensity on the performance of Gurney-flap equipped wind-turbine blades. Wind Eng; 20(2):93–106.

50 W.A.Timmer and R.P.J.O.M.van Rooij, 2003 "Summary of the Delft University Wind Turbine Dedicated Airfoils", ASME Journal of Solar Energy Engineering, Vol. 125, 488-496.

51 G. Pechlivanoglou, C.N. Nayeri and C.O. Paschereit, 2011 "Performance optimization of Wind Turbine Rotar with Active Flow Control", Proceedings of ASME Turbo Expo 2011; GT2011-45493.

52 Peter Fuglsang, Christian Bak, Mac Gaunaa and Ioannis Antoniou, 2004 "Design and Verification of the Risø-B1 Airfoil Family for Wind Turbines", ASME Journal of Solar Energy Engineering, Vol. 126, 1002-1010.

53 Nengsheng Bao, Haoming Ma, Zhiquan Ye., 2000 "Experimental Study of Wind Turbine Blade Power Augmentation Using Airfoil Flaps, including the Gurney Flap", Wind Engg.,Vol. 24, No. 1.

54 Zhang Xu, Qian Wang, Geng Dai, Hongfei Tan and Yingjie Zhong, 2011 "Study on improvement in aerodynamic performance of Vertical Axis Wind Turbine using Gurney flap", Mechanic Automation and Control Engineering (MACE), Second International Conference. pp. 6884–6887.

55 Zhao, W.L., Liu, P.Q., Zhu, J.Y. and Qu, Q.L, 2011 "Numerical investigation of flow control on performance enhancing by mounting gurney flaps of a large horizontal wind turbines", Artificial Intelligence, Management Science and Electronic Commerce (AIMSEC), 2nd International Conference pp. 4111 – 4114.

56 Zhu Wen-xiang, Yu Guo-liang, Tian Mao-fu and Shen Zhen-hua, 2008 **"**Experimental investigation on performance enhancing for wind turbine by mounting Gurney flap to the blade", Renewable Energy Resources, 2008-02.

57 Cahnin Tongchitpakdee, Sarun Benjanirat and Lakshmi N. Sankar, 2006 "Numerical Studies of the Effects of Active and Passive Circulation Enhancement Concepts on Wind Turbine Performance", ASME J of Solar Energy Eng. Vol. 128, pp. 432-444.

7.MAILING ADDRESS

M. Suresh,N. Sitaram
Thermal Turbomachines Laboratory, Department of Mechanical Engineering
IIT Madras, CHENNAI – 600 036, India
Phone: 91 44 2257 4965
E-mail: suremreddy@gmail.com